

Excitation Decay Pathways of Lhca Proteins: A Time-Resolved Fluorescence Study

Janne A. Ihalainen,^{*,†} Roberta Croce,[‡] Tomas Morosinotto,^{§,⊥} Ivo H. M. van Stokkum,[†] Roberto Bassi,^{§,⊥} Jan P. Dekker,[†] and Rienk van Grondelle[†]

Faculty of Sciences, Department of Physics and Astronomy, Vrije Universiteit, De Boelelaan 1081, 1081 HV Amsterdam, The Netherlands, Istituto di Biofisica, CNR, Trento, c/o ITC via Sommarive 18, 38100 Povo, Trento, Italy, Dipartimento Scientifico e Tecnologico, Università di Verona, Strada Le Grazie, 15–37134 Verona, Italy, and Université Aix-Marseille II, LGBP, Faculté des Sciences de Luminy, Département de Biologie, Case 901, 163 Avenue de Luminy, 13288 Marseille, France

Received: April 14, 2005; In Final Form: September 9, 2005

Light-harvesting complex I (LHCI), which serves as a peripheral antenna for photosystem I (PSI) in green plants, consists mainly of four polypeptides, Lhca1–4. We report room temperature emission properties of individual reconstituted monomeric Lhca proteins (Lhca1, -2, -3, and -4) and dimeric Lhca1/4, performed by steady-state and time-resolved fluorescence techniques. The emission quantum yields of the samples are approximately 0.12, 0.085, 0.081, 0.041, and 0.063 for Lhca1, -2, -3, -4, and the -1/4 dimer, respectively, which is considerably lower than the value of 0.22 found for light-harvesting complex II (LHCII), the main peripheral antenna complex of photosystem II in green plants. The decay components of LHCI proteins can be divided in two categories: Lhca1 and Lhca3 have decay times of 1.1–1.6 ns and 3.3–3.6 ns, and Lhca2 and Lhca4 have decay times of 0.7–0.9 ns and 3.1–3.2 ns. These categories seem to correlate with the pigment composition of the samples. All decay times are faster than that observed previously for LHCII. When the absolute emission yields and the lifetimes of the Lhca samples are combined, the overall emission properties of the individual Lhca proteins are expressed in terms of their emitting dipole moment strength. In the samples without extreme red states, that is, Lhca1 and Lhca2, the emitting dipole moment has a value close to unity (relative to monomeric chlorophyll in acetone), which is similar to that for LHCII, whereas, in the samples with the red-most state (F-730), that is, Lhca3, -4, and the -1/4 dimer, the emitting dipole moment has a value less than unity (0.6–0.8), which can be explained by mixing the red-most (exciton) state with a dark charge-transfer state, as suggested in previous PSI red pigment studies. In addition, we find a lifetime component of ~ 50 –150 ps in all red-pigment-containing samples, which cannot be due to “slow” energy transfer, but is instead assigned to an unrelaxed state of the pigment–protein, which, on this time-scale, is converted into the final emitting state.

Introduction

Light-harvesting complex I (LHCI) is the peripheral antenna of photosystem I (PSI) in green plants and algae, and it collects and transfers excitation energy to the reaction center of PSI, where it is trapped in the form of a stable charge separation. In green plants, LHCI consists mainly of four polypeptides, Lhca1–4.¹ Furthermore, Lhca5 may be present, which contributes a minor increase in the antenna size.^{2,3} LHCI is attached in dimeric form at one side of the PSI core antenna.^{4,5}

The Lhca polypeptides belong to the so-called Lhc-supergene family, and they all bind chlorophyll a and b (Chl *a* and Chl *b*) molecules and carotenoids.^{2,6} All Lhca proteins show a high sequence homology with the Lhcb proteins, which are the peripheral antenna proteins of photosystem II (PSII). The pigment binding sites are considered to be similar for all Lhc proteins. The structure of the main peripheral light-harvesting

complex of PSII, LHCII, is known with 2.72 Å resolution,⁷ and its spectroscopic properties and excitation dynamics are characterized in detail.^{8–10}

Despite the similar pigment arrangement, some of the spectroscopic properties among Lhca proteins and between Lhca and Lhcb proteins are significantly different. The most obvious differences between the Lhca and Lhcb proteins appear in the low-temperature emission spectra, where Lhca proteins show a considerably red-shifted emission compared with that of the Lhcb proteins. The red-most emission of Lhca3 and Lhca4 is located at ~ 730 nm at cryogenic temperatures,¹¹ whereas in all Lhcb proteins it is ~ 680 nm. Thus, the lowest singlet excited state of the Chl's in these Lhca proteins resides at much lower energy than does that of Lhcb proteins. The red-most states in the PSI antenna are even lower than the main absorption of the reaction center of PSI (700 nm). It has been shown that these red states prolong the overall trapping time of native PSI–LHCI particles in green plants^{12,13} and in PSI core particles from cyanobacteria.^{14,15}

Because isolated LHCI preparations from green plants usually consist of two or three types of dimeric Lhca complexes, the spectroscopic studies on isolated LHCI have revealed information averaged over the Lhca proteins.^{16–21} Separating the Lhca proteins in their native form has turned out to be very cumbersome

* Corresponding author. E-mail: janihal@nat.vu.nl. Fax: +31205987999. Present address: the University of Zürich, Institute of Physical Chemistry, Winterthurerstrasse 190, 8057 Zürich, Switzerland. Alternate e-mail: jihala@pci.unizh.ch.

[†] Vrije Universiteit.

[‡] Istituto di Biofisica, CNR.

[§] Università di Verona.

[⊥] Université Aix-Marseille II.

because all Lhca proteins have similar biochemical properties. Researching individual Lhca proteins became possible once they could be reconstituted *in vitro*, and mutants of Lhca became available.^{11,22–25} Since then, our knowledge of the pigment composition, protein–protein interactions, and (steady-state) spectroscopic properties of individual Lhca proteins has increased considerably.^{11,23–27}

Until now, only a few studies on individual Lhca proteins have appeared that describe the excitation transfer kinetics among the Chl molecules and the excitation decay processes.^{28–30} Now that the reconstitution (and mutation) procedure of the individual Lhca proteins has been established, it is clear that more information on the excitation (decay) dynamics among the pigments in Lhca proteins will become available.³¹ The observations made with such “small” particles can then be linked to the overall excitation dynamics taking place in the green plant PSI–LHCI complexes, which will lead to a more complete picture of the excitation pathways from the peripheral antenna via the core antenna to the reaction center in green plant PSI. Because the PSI–LHCI particle is a large pigment–protein complex with ~170 chlorophylls and more than 30 carotenoids,^{5,32} detailed information on the excitation energy pathways is difficult to obtain by studying PSI–LHCI particles only.

In this paper, we study the room-temperature fluorescence decay properties of four monomeric Lhca proteins (Lhca1–4) and a dimeric Lhca1/4 protein, by using a Streak camera setup with about 5 ps time resolution. We show that the excitation decay takes place biphasically in all Lhca proteins and that the decay times depend both on the pigment composition and on the red pigment content of the proteins. We also show that in the samples containing red pigments, that is, in the monomeric Lhca2–4 and dimeric Lhca1/4 complexes, the formation of the final excited state occurs on the order of hundreds of picoseconds, which cannot be due to a typical energy transfer process, but most likely reflects a small structural rearrangement in the protein following the excitation.

Materials and Methods

The samples were prepared as described by Morosinotto *et al.* in 2003¹¹ and diluted with a buffer containing 10 mM Hepes (pH 7.6) and 0.03% β -DM. For the steady-state measurements the samples were placed in a 1 \times 0.4 cm cuvette, and, for the time-resolved measurements, all of the samples were placed in a 0.5 \times 0.5 cm cuvette, which was shaken during the measurement.

The steady-state absorption spectra and fluorescence emission spectra were detected with commercial spectrophotometers (Perkin-Elmer, Lambda 40 and Jobin Yvon, Fluorolog, respectively). After the emission spectra were normalized to the same excitation power, the emission yields of the samples were determined by integrating the emission spectrum of the sample and using the emission of Chl *a* in acetone with a yield of 0.3 as a reference.³³

The time-resolved measurements were performed with a Streak camera setup. In short, excitation pulses of 486 nm (~100 fs) with vertical polarization were generated using a titanium: sapphire laser (Coherent, VITESSE) with a regenerative amplifier (Coherent, REGA), a double pass optical parametric amplifier (Coherent, OPA), and a Berek compensator. The repetition rate was 50 kHz with a pulse energy of 4 nJ in the sample, which resulted in less than 20% excited proteins per pulse. The fluorescence was detected at a right angle with respect to the excitation beam through a polarizer at a magic angle using

TABLE 1: Pigment Composition of Reconstituted Lhca Monomers^{a,b}

sample	Chl total	Chl <i>a/b</i>	lutein	viola	β -car/neo
Lhca1	10	4.0	1.5	1.1	0.2
Lhca2	10	1.9	1.5	0.5	
Lhca3	10	5.5	1.7	0.6	0.4
Lhca4	10	2.4	1.7	0.4	
Lhca1/4	20	3.0	2.4	1.6	0.8

^a Taken from refs 6 and 11. ^b viola = violaxanthin, β -car = β -carotene, neo = neoxanthin.

a Chromex 250IS spectrograph and a Hamamatsu C5680 synchroscan streak camera. The streak images were recorded with a cooled Hamamatsu C4880 CCD camera. The exposure times per image were 5–10 min and 2–6 min for the 500 ps and 2 ns time bases, respectively. The detected streak images, which showed a whole time-resolved fluorescence spectrum of the Chl *a* and Chl *b* molecules of the samples, were analyzed globally from 635 to 810 nm with 8 nm resolution, and the decay-associated spectra (DAS) were estimated.^{34,35} The instrument response function was modeled as a Gaussian with FWHMs of about 5 and 15 ps for the 500 ps and 2 ns time bases, respectively. In addition, the data was modeled by using a so-called target analysis method.^{34,35}

Results

Steady-State Absorption and Emission. Biochemical and steady-state spectroscopic analyses of the reconstituted Lhca1–4 samples used in this study have been reported in detail.^{6,11,24,25,27} The pigment composition of each of the particles is shown in Table 1.^{6,11} Room-temperature steady-state absorption and emission spectra of the samples are presented in Figure 1.

In absorption (Figures 1A and 1C), the Q_y -transitions of the “bulk” Chl *a* molecules have their maxima at 680, 679, 679, 675, and 677 nm for Lhca1, -2, -3, -4, and the -1/4 dimer, respectively. A red tail (around 690–715 nm) in the absorption can be observed for the Lhca2, -3, -4, and -1/4 samples. The blue-most red pigment absorption is observed for the Lhca2 samples, which is in line with the low-temperature experiments, in which Lhca2 has the blue-most absorption and emission out of the Lhca2, -3, -4, and -1/4 samples.^{24,27} Because the red tail is structureless at room temperature, the position of the red-most band is estimated, to a certain extent, only from the 4 K absorption spectra. For Lhca1, the red pigment absorption of the samples is only seen as a very weak tail of the main absorption band.

Figure 1B shows the steady-state emission spectra of the samples together with the emission spectrum of Chl *a* in acetone. The spectra are normalized to the excitation density (i.e., the number of absorbed photons), except for the free Chl *a* spectrum, which is normalized to half the excitation density and scaled down in such a way that the maximum of the free Chl *a* emission has a value of 0.15, which is approximately half of its real quantum yield, 0.3.³³ At room temperature, the strongest emission originates from emission of the bulk Chl *a* molecules, and the maxima of the samples are located at about 683, 683, 681, 678, and 681 nm for Lhca1, -2, -3, -4, and the -1/4 dimer, respectively (Figure 1D). These emission maxima follow the same order as that observed for the absorption maxima of the samples (Figure 1A, see above). Depending on the red pigment energy and content of the samples, a red emission band can be observed. As in the case of the absorption, a clear maximum of the red band cannot be determined. At low temperatures, the red-most emission is observed at about 701–702 nm for Lhca1

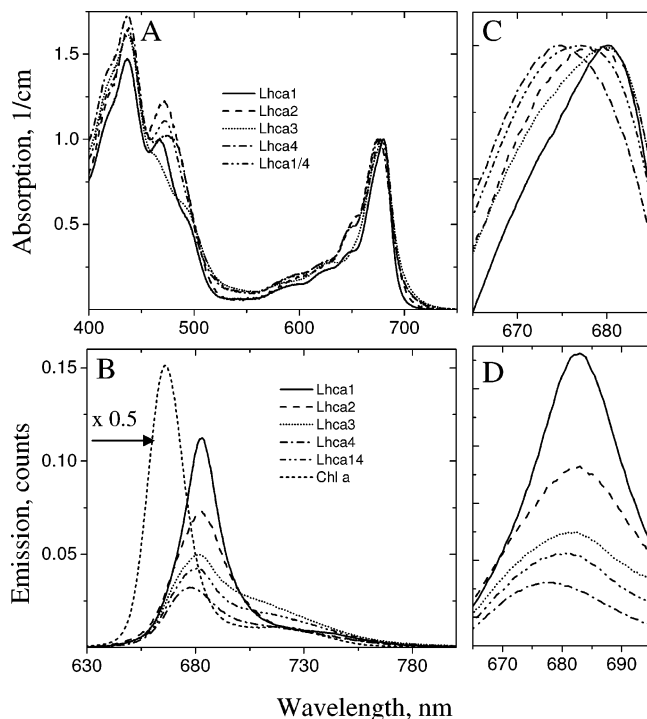


Figure 1. Room-temperature absorption spectra (A) and emission spectra upon 430 nm excitation (B) of the Lhca monomers (Lhca1–4), the Lhca1/4 dimer, and Chl *a* diluted in acetone. (C) A close-up of the Q_y -absorption band of the spectra shown in (A). (D) A close-up of the Q_y -emission band of the spectra shown in (B). The absorption spectra are normalized to their Q_y -absorption maximum around 680 nm, and the emission spectra are normalized according to their excitation power; that is, the yields are comparable with each other. For clarity, the Chl *a* emission spectrum is multiplied by a factor of 0.5.

TABLE 2: Collection of the Decay Lifetimes and Integrated Relative Amplitudes of the Lhca Monomers and the Lhca1/4 Dimer^{a,b}

sample	$\tau_1(\text{ns})/A_{\text{rel}}$	$\tau_2(\text{ns})/A_{\text{rel}}$	$\tau_3(\text{ns})/A_{\text{rel}}$	τ_{ave}
Lhca1	1.65/0.45	3.34/0.55	2.58	
Lhca2	0.06/0.13	0.8/0.45	2.91/0.42	1.58
Lhca3	0.19/0.1	1.30/0.58	3.59/0.32	1.92
Lhca4	0.11/0.16	0.72/0.54	3.21/0.29	1.32
Lhca1/4	0.05/0.12	0.68/0.45	2.84/0.43	1.54

^a Obtained from global analysis (see the spectral forms of the components from Figure 3). ^b The average lifetime (τ_{ave}) is calculated according to $(\sum A_n \times \tau_n)$.

(a shoulder) and Lhca2 and at 725, 732, and 732 nm for Lhca3, -4, and the -1/4 dimer, respectively.^{11,24,27} When compared with the emission yield of 0.3 for Chl *a* in acetone, the room-temperature emission yields of the samples are about 0.12, 0.085, 0.081, 0.041, and 0.063 for Lhca1, -2, -3, -4, and the -1/4 dimer, respectively, (see Materials and Methods and also Table 4). The emission yield of the Lhca monomers inversely follows the red pigment content; that is, the highest yield is observed for Lhca1 and the lowest for Lhca4 (Table 4 and see also Discussion). The Lhca1/4 dimer has a slightly higher yield than does the Lhca4. Another clear observation is that, on average, the quantum yield of LHCI proteins is almost four times lower than that of free Chl *a* and is also considerably lower than the value of 0.22 found for LHCI.³⁶ This is in line with the fact that LHCI has a major emission lifetime of about 4 ns at room temperature,³⁶ whereas in the Lhca proteins, the fluorescence decay is faster (see below).

TABLE 3: (A) Excitation Proportions of the Branching Resulting from the Target Analysis of the Lhca Monomers and Lhca1/4 Dimer; (B) Lifetimes of the Compartments Resulting from the Target Analysis of the Lhca Monomers and Lhca1/4 Dimer^a

(A)					
	P_1	P_2	P_3	P_4	
Lhca1	0.55	0.45	0.02	0.98	
Lhca2	0.58	0.42	0.28	0.72	
Lhca3	0.45	0.55	0.23	0.77	
Lhca4	0.43	0.57	0.30	0.70	
Lhca1/4	0.58	0.42	0.22	0.78	
(B)					
	τ_1	τ_2	τ_3	τ_4	τ_5
Lhca1	0.6 ps	4 ps	116 ps	1.6 ns	3.3 ns
Lhca2	0.7 ps	5 ps	78 ps	0.9 ns	3.1 ns
Lhca3	0.8 ps	5 ps	126 ps	1.1 ns	3.6 ns
Lhca4	0.8 ps	6 ps	108 ps	0.7 ns	3.2 ns
Lhca1/4	0.5 ps	6 ps	38 ps	0.7 ns	2.7 ns

^a The model is shown in Figure 4.

TABLE 4: Collection of the Fluorescence Emission Quantum Yield,^a the Average Lifetimes,^b and the Calculated Emitting Dipole Moments (μ^2)^{c,d}

	yield (%)	$\tau_{\text{ave}}(\text{ns})$	$k_{\text{rad}}(1/\text{ns})$	n	ν_{mean}	m^2
Lhca1	12.0	2.58	0.047	1.52	14477	0.91 ± 0.1
Lhca2	8.5	1.58	0.054	1.52	14425	1.06 ± 0.1
Lhca3	8.1	1.92	0.042	1.52	14219	0.87 ± 0.1
Lhca4	4.1	1.32	0.031	1.52	14237	0.64 ± 0.2
Lhca1/4	6.3	1.54	0.041	1.52	14216	0.84 ± 0.1
LHCII ^e	21.6	4.00	0.054	1.52	14650	1.01
Chl <i>a</i>	30	6.10	0.049	1.36	14828	1.00

^a From Figure 1. ^b Taken from Table 2; these values are then converted to radiative rate, k_{rad} . ^c According to the equation $k_{\text{rad}} = n16\pi^3\nu^3/3\epsilon_0hc^3|\bar{\mu}|^2$, in which n is the refractive index of the medium, ϵ_0 is the vacuum dielectric constant, h is Planck's constant, c is the speed of light, and ν is the emission frequency taken as a mean frequency of the emission spectra (see more details in ref 36). ^d The emitting dipole moments of the samples are normalized to the emitting dipole moment of the Chl *a* molecule diluted in acetone. ^e In the case of LHCI, the values presented in ref 36 have a refractive index of 1.52 instead of 1.31.

Time-Resolved Fluorescence. We studied the time-resolved emission properties of the samples by using streak camera detection after short laser pulse excitation with a wavelength of 486 nm, which mainly excites carotenoids and Chl *b* molecules with a ratio of about 60/40,³¹ respectively. Figure 2 shows few fluorescence decay traces at the main emission band and at the red emission band of monomeric (Lhca1–4) particles and the dimeric Lhca1/4 particles taken from the detected streak images. From the traces it can be seen that the overall decay times qualitatively follow the emission yields observed from the steady-state experiment; that is, the Lhca1 has a longest decay time and the Lhca4 has the shortest. From the traces it is also clear that, at early times of the emission, excitation energy transfer takes place, and, subsequently, the fluorescence decays multiexponentially. To solve the excitation kinetics taking place in the ps and ns range in detail, a global analysis of the data was performed. The results, that is, the DAS of monomeric (Lhca1–4) particles and the dimeric Lhca1/4 particles, are shown in Figure 3. The first, less than 1 ps component (thin solid line in Figure 3) shows positive features (i.e., decay of excitation) at Chl *b* emission wavelengths and overall negative features (i.e., rise of excitation) in the Q_y -region of Chl *a* molecules. This component describes the excitation energy transfer from carotenoids and Chl *b* molecules to Chl *a* molecules, which mainly takes place on a subpicosecond time-

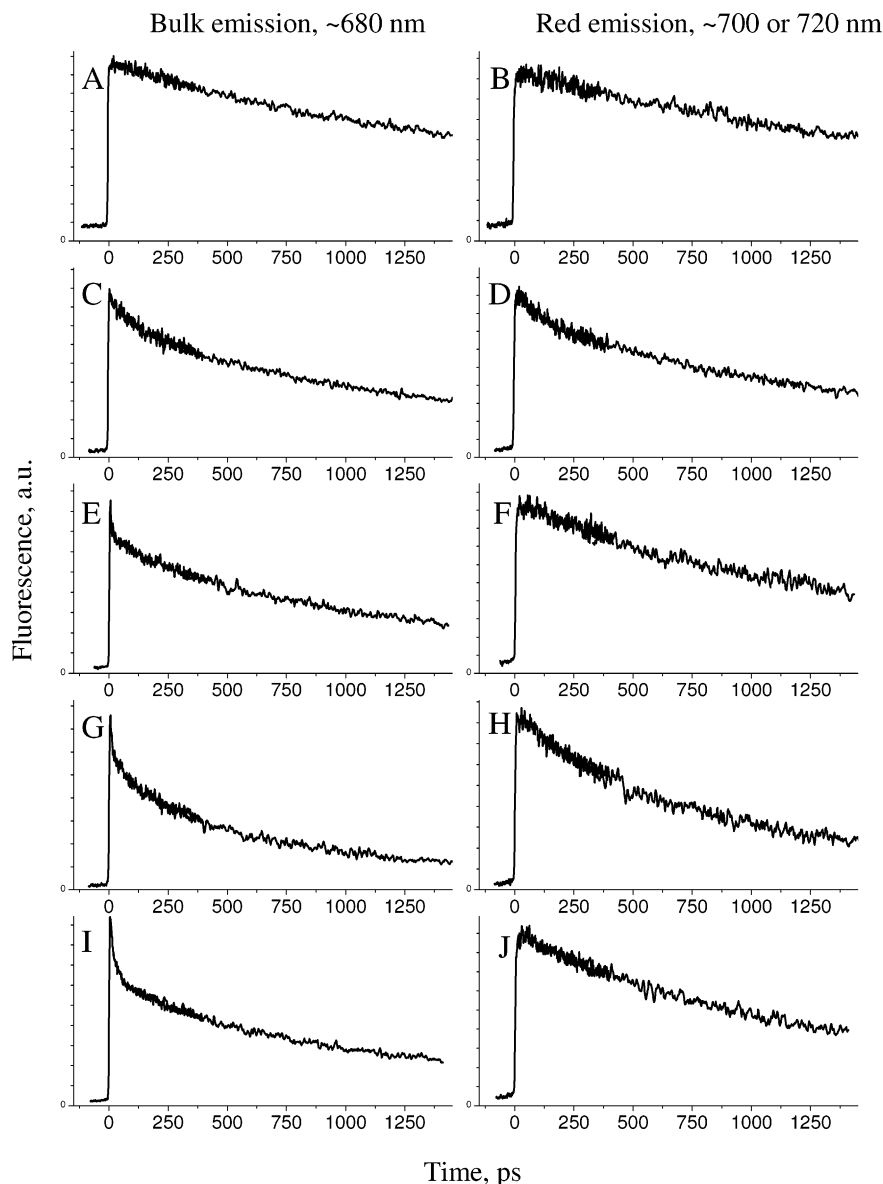


Figure 2. Fluorescence decay traces of Lhca monomers and the Lhca1/4 dimer after 486 nm excitation at room temperature: (A) Lhca1 at 680 nm, (B) Lhca1 at 700 nm, (C) Lhca2 at 680 nm, (D) Lhca2 at 700 nm, (E) Lhca3 at 680 nm, (F) Lhca3 at 720 nm, (G) Lhca4 at 680 nm, (H) Lhca4 at 720 nm, (I) Lhca1/4 at 680 nm, and (J) Lhca1/4 at 720 nm. The fluorescence traces have a 5-ps time resolution up to ~ 200 ps and a 15-ps time resolution at later times.

scale.^{20,30,31} Because this time-scale is below the time resolution of our experiment (by about 5 ps), the time constant needs to be taken with caution. In the samples in which red pigments exist, that is, Lhca2–4 and the -1/4 dimer, the excitation equilibration component between bulk and red pigments, with a rather conservative spectral shape, has a lifetime of about 5–6 ps in all samples. As mentioned above, the excitation energy of the red-most state varies between the samples, but this is not reflected in this bulk-to-red equilibration time.

All samples required more than one decay lifetime to explain their time-resolved fluorescence emission. More than 80% of the excitations decayed in the nanosecond regime in all samples, and in the case of samples with red pigments, that is, Lhca2–4 and the -1/4 dimer, 20% of the excitations decayed in a 100 ps regime (Figure 3, see text below). The nanosecond-decay components can be divided into two categories: Lhca1 (Figure 3A) and Lhca3 (Figure 3C), with decay times of 1.3–1.6 ns and 3.4–3.6 ns, and Lhca2 (Figure 3B) and Lhca4 (Figure 3D), with decay times of 0.7–0.8 ns and 2.9–3.2 ns. These categories seem to correlate with the pigment composition of the samples

(Table 1): the faster decay times were observed in samples with higher Chl *b* and lower carotenoid content. The decay lifetimes and their integrated amplitudes are listed in Table 2, which can be used to calculate the average decay times for each sample. By comparing the values from Table 2 and the steady-state emission spectra in Figure 1, the averaged emission lifetimes correlate reasonably with the quantum yields of the samples, and it is clear that in Lhca3 and Lhca4, which bind the red-most pigments, the 1 ns decay component is more dominating compared to the 3 ns decay component. On the other hand, for Lhca1 and Lhca2, the 3 ns component contributes to either slightly more (Lhca1) or less (Lhca2) than 50% of the overall excitation decay (Figure 3 and Table 2). The main decay rates of Lhca1 are rather similar to those reported by Melkozernov et al.²⁸ For Lhca4, the longer decay lifetime of our study (3.2 ns) is almost two times longer than the value reported by Melkozernov et al.,²⁸ whereas, in our case, the long lifetime of the Lhca1/4 dimer (2.8 ns) is about 40% longer. On the other hand, the relative contributions of the decay lifetimes to the total emission differ quite drastically between this study and

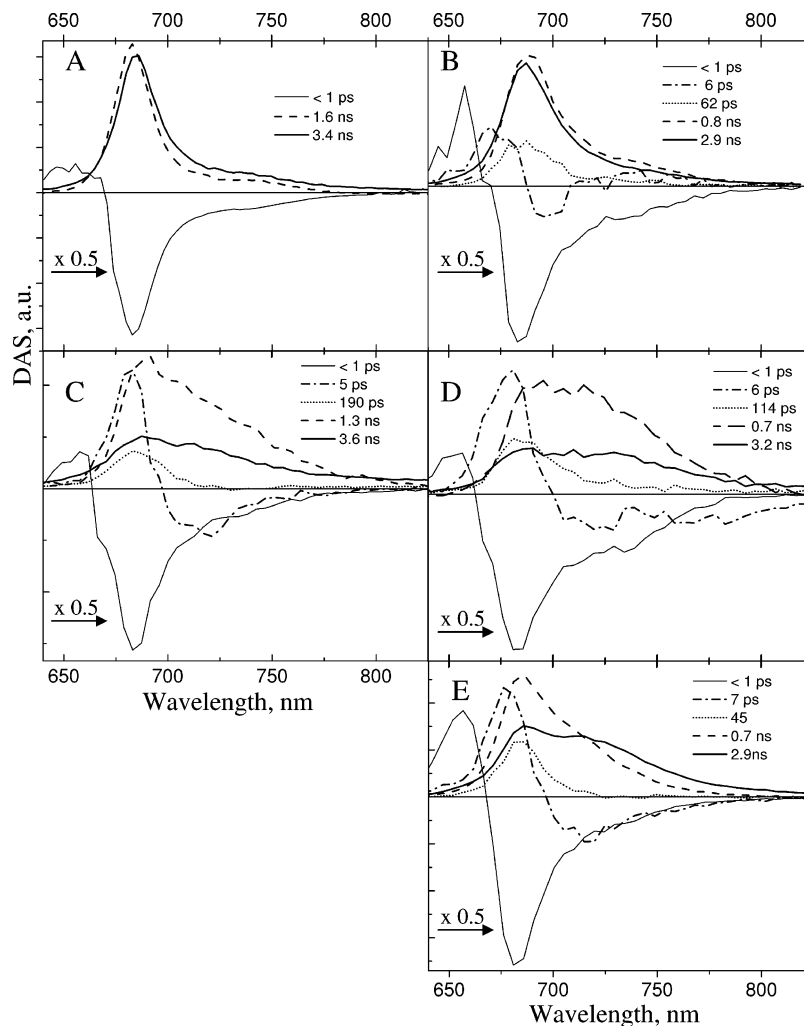


Figure 3. DAS of Lhca monomers and the Lhca1/4 dimer after 486 nm excitation at room temperature: (A) Lhca1, (B) Lhca2, (C) Lhca3, (D) Lhca4, and (E) Lhca1/4.

the study performed by Melkozernov et al.²⁸ In the latter, the major decay component is the 1 ns decay, which also is the major contributor to the steady-state emission, whereas, in our study, the 3 ns component is the most dominant phase for the steady-state emission (with a relative contribution of about 0.6–0.8 in all samples, $\tau_3 A_3 / \tau_{\text{ave}}$, taken from Table 2). The reason for these discrepancies may be due to the different sample preparation or to the different reconstitution methods of the complexes, which results in slightly different pigment/protein ratios.^{11,22}

The Lhca1/4 dimer has main decay components that are similar to those of the Lhca2 and Lhca4 monomers, and the overall kinetics of the Lhca1/4 dimer resembles that of native LHCI samples,^{20,28} which suggests that Lhca2/3 should have excitation dynamics similar to those of Lhca1/4. This statement, however, needs to be confirmed once the isolated Lhca2/3 dimer becomes available.

In addition to the nanosecond decay processes, in Lhca2, -3, -4 and the -1/4 dimer (i.e. samples with red pigments), after equilibration between bulk and red pigments, we observed a decay process with a lifetime of about 50–200 ps with positive features between 670 and 690 nm and without a pronounced negative feature in the red pigment region (dotted lines in Figure 3). This means that an apparent loss of excitation takes place in the bulk pigments, and no gain of excitation on the red pigments can be observed, implying that this is not a “traditional” energy-transfer component. On the other hand, the 50–

200 ps spectrum deviates from a typical emission spectrum of Chl *a* molecules in the sense that it has less contribution from the vibronic wing, especially in the cases of Lhca3 and the Lhca1/4 dimer. In the following section, we describe this component as an intermediate phase preceding the final decay state by using a branched target analysis for the observed data.

Target Analysis. So far, we have treated the time-resolved fluorescence data basically without a priori information, and we have fitted the data globally with as many decay components as required for sufficient description of the data. We constructed a model that gives the physical spectra and decay and rise times of each compartment and describes the connectivity between the compartments. Thus, the model *quantitatively* determines the proportions of each decay and energy-transfer channel of the system observed by time-resolved fluorescence. Such an approach is called a target analysis. A comprehensive description of target analyses of time-resolved spectroscopic data can be found elsewhere.^{34,35} In this case, the number of components observed in the global analysis dictates the number of compartments in the target analysis. The connectivity between the compartments (i.e., the arrows between the compartments) is assumed to be as simple as possible to describe the data, but, at the same time, the shape of the emission spectra of the compartments needs to be physically acceptable, that is, either typical Chl *a* emission spectra or red chlorophyll-type of spectra, in which the vibronic part of the Chl *a* emission is replaced by a broad, structureless emission from the red pigments. The

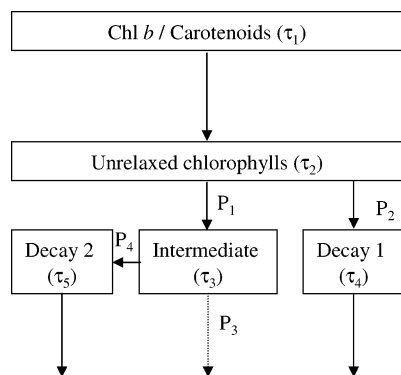


Figure 4. The model used in the target analysis. P_n expresses the proportional values of the branching of excitation, and τ_n represent the lifetimes of the compartments. The values are shown in Table 3.

modeled branching proportions (i.e., the weight of excitation for each compartment) were accepted when the areas of the emission spectra of the compartments were the same (within an error of 5%).

The model used for all of the samples is shown in Figure 4. To describe the time evolution of the spectra, two separate decay pathways following the population of Soret states and unrelaxed bulk states are needed, one of which is the so-called “Intermediate” → “Decay 2” route, and the other is the “Decay 1” channel (Figure 4). In fact, in the target analysis, it is indistinguishable whether the Intermediate compartment leads to a longer or shorter decay because both models give the same residuals with corresponding spectra; however, we tentatively assign the Intermediate state to the longer decay time for all samples. It is clear, however, that the Intermediate compartment cannot be a pure decay channel because, in that case, the target analysis results in a nonphysical emission spectrum, which lacks the vibronic part or red-emitting part (data not shown). The observed values, in terms of the branching proportions and the lifetimes of the compartments, are given in Table 3, and the spectra of the compartments are shown in Figure 5. We note that, for the sake of clarity, we used the same model for all of the samples, although, for Lhca1, the scheme could have been much simpler, and the states “Unrelaxed chlorophylls” and “Intermediate” are basically virtual.

In the target analysis, the first spectrum (thin solid line in Figure 5), which originates from Chl *b* molecules, was set to zero at all wavelengths longer than 665 nm, and its amplitude as well as its lifetime are imprecise because of the time resolution of our experiment. The second spectrum (dot–dashed line in Figure 5), which we call “Unrelaxed chlorophylls”, basically shows a bulk Chl *a* emission spectrum of the samples. The expression “unrelaxed” is chosen because, in samples with red pigments (Lhca2, -3, -4 and the -1/4 dimer), the blue side of the spectrum is considerably more blue-shifted than the spectrum calculated using the Stepanov relation between the absorption and emission spectra (not shown). This means that this compartment describes Lhca proteins in a nonequilibrated excited state. The equilibration time (i.e., the sum of forward and backward reaction times) between the bulk and the red pigments of the Lhca proteins is about 4–6 ps (Table 3B). Similarly, with the observation from global analysis, the lifetime of this compartment is insensitive to the energy of the red chlorophylls or to the overall amount of pigments. Then the two separate excitation decay pathways follow, one of which is the so-called Intermediate → Decay 2 route, and the other is the Decay 1 channel (Figure 4). The lifetimes of the Decay compartments follow the same categories observed in the global

analysis. In the samples of Lhca3, -4, and -1/4, the emission spectra of the Intermediate compartment (dotted line in Figure 5.) show considerably stronger amplitude around 685 nm compared to the spectra of the Decay 2 compartment (solid line in Figure 5). This indicates a loss of emission from the bulk pigments, as was concluded earlier from the global analysis. The spectra of the Decay 1 compartment (dashed line in Figure 5) show a rather strong contribution from the red pigments. The trend in the red contribution in the spectra obtained from the target analysis for each sample (Figure 5) follows the observations from the steady-state spectra at room temperature (Figure 1) and at low temperatures (see above); that is, Lhca4 shows the red-most spectra, and Lhca1 shows the least-red spectra.

From Table 3A it can be seen that when the F702 is the red-most state (Lhca1 and Lhca2), a higher proportion (about 55%) follows a route toward the longer lifetime (Intermediate → Decay 2), whereas in the case of Lhca3 and Lhca4, a higher proportion decays via Decay 1. In the case of the Lhca1/4 dimer, the situation resembles that of Lhca1 and Lhca2. By multiplying the decay rates of the particular compartment ($1/\tau_c$ from Table 3B) with the branching proportions (Table 3A), the rise times of the Intermediate and Decay 1 compartments can be determined to be between 9 and 14 ps. Similarly, the rise-time of the Decay 2 compartment from the Intermediate is found to range between 110 and 160 ps in the monomers and is about 50 ps in the Lhca1/4 dimer. The 20–30% loss of excitation of the intermediate state in the samples of Lhca2, -3, -4, and -1/4 gives then a time constant for the deactivation process of 280–550 ps for the monomers and of about 170 ps for the Lhca1/4 dimer.

Discussion

In this study, we investigated the fate of excitation energy in the monomeric Lhca proteins (Lhca1, -2, -3, and -4) and in the dimeric Lhca1/4 protein after excitation at 486 nm (which mainly excites carotenoid and Chl *b* molecules). By comparing the main decay lifetimes (Figure 3 and Table 2) and the pigment composition of the monomers (Table 1), we observed two decay patterns that reflect the pigment composition of the samples. The Lhca1 and Lhca3 samples, which have a lower Chl *b* content and bind an “extra” carotenoid, which in most cases is either β -carotene or neoxanthin (Table 1), both have main decay times of more than 1 ns. In contrast, the Lhca2 and Lhca4 samples exhibit the “faster” decay (Decay 1 in the target analysis) of less than 1 ns, and the final decay is \sim 3 ns. These samples have a higher Chl *b* and lower carotenoid content.

It is well known, that in a protein environment the excited-state lifetimes of chlorophylls can be shorter than that of those in solution (\sim 6 ns, Table 4). Electron transfer (or trapping) processes may shorten the excited-state lifetimes of these pigments by orders of magnitudes. However, in antenna proteins, electron-transfer processes do not take place, and therefore, pigment–pigment coupling (both chlorophyll–chlorophyll and carotenoid–chlorophyll coupling) and pigment–protein coupling are the main factors leading to the shortening of the excited-state lifetimes. In the case of chlorophyll–chlorophyll coupling, or exciton coupling, the higher delocalization length of a state either lengthens or shortens the fluorescence lifetime, depending on the orientation of the pigments.³⁷ Because of the very short lifetime of the excited states of carotenoids, even a small carotenoid–chlorophyll coupling (on the order of a few wavenumbers) may drastically shorten the excited-state lifetime of chlorophylls.^{8,38} The coupling of the excited state with a charge-transfer state (which can be categorized as pigment–

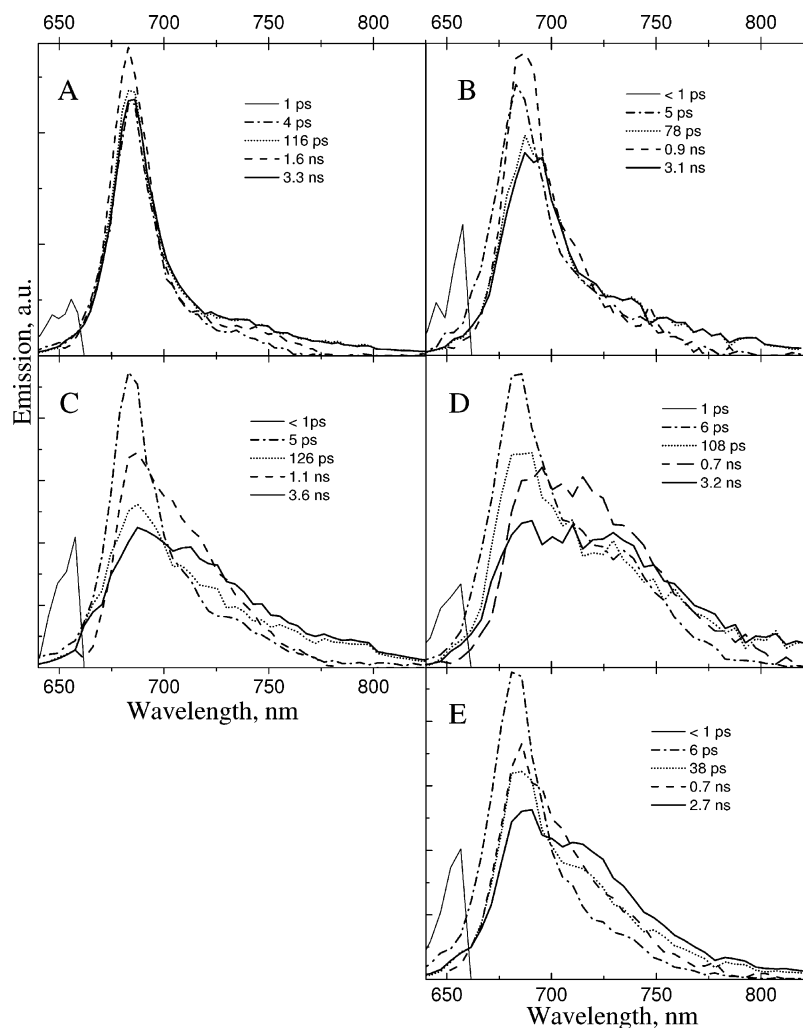


Figure 5. The spectra of the compartments (species-associated spectra) of the Lhca monomers Lhca1 (A), Lhca2 (B), Lhca3 (C), and Lhca4 (D) and the Lhca1/4 dimer (E) estimated from target analysis using the model from Figure 4. The relation between the compartments (Figure 4) and the spectra is as follows: thin solid line = Chl *b*/carotenoids; dot-dashed line = Unrelaxed Chl *a*; dotted line = Intermediate; long dashed line = Decay 1; thick solid line = Decay 2. The time constants represent the decay times of each compartment (see also Table 3B).

pigment coupling) can also affect the lifetime, but in both directions, depending on the lifetime of the charge-transfer state (T. Renger, personal communication). However, in most practical cases, the lifetime is drastically shortened. Recently, in thylakoid membranes under conditions of maximum, steady-state feedback deexcitation, upon Chl *a* excitation, a 11 ps rise component was observed at 1000 nm, in the region where one might expect to see a formation of a carotenoid radical.³⁹ The authors suggested that the rise is due to the formation of a charge-transfer state of a zeaxanthin–chlorophyll pair, which is then responsible for excess energy dissipation in thylakoid membranes in green plants. In principle, the protein environment will also affect the excited-state lifetime of chlorophylls; in most cases, it will shorten the lifetimes. One, rather extreme example was observed in a study of the Cytb₆f complex, which binds one isolated chlorophyll molecule, in which the pigment–protein coupling reduced the excited-state lifetime of the chlorophyll to 215 ps,⁴⁰ probably because of electron transfer to a nearby aromatic amino acid.⁴¹

Most likely, all of the above-mentioned effects influence the lifetimes of the studied Lhca proteins. The red pigments of LHCI have been shown to carry a large Huang–Rhys factor (on the order of 3), which leads to strong (in)homogeneous broadening and large Stokes' shift.^{18,19} These observations can be rationalized by a mixture of the red-most (exciton) state with a charge-

transfer state because a polar state couples strongly to the vibrations of the environment.⁴² On top of that, various carotenoid–chlorophyll interactions between red pigments and carotenoids were observed in a magnetic resonance study with Lhca proteins.⁴³ However, assignment of the precise contribution of each of these effects requires further investigation with a set of samples in which the pigment composition or the amino acid environment of the emitting pigments has been slightly modified. In fact, even the multiphase decay of the samples is puzzling. It is possible that, because of some (small) differences in the proteins in the ensemble, the decay pathway can be either intermediate-to-decay or “pure” decay, and then, with a certain contribution, the above-mentioned factors affect the fluorescence lifetimes of the samples.

Now that we have expressed the total emission yields and lifetimes of the Lhca samples, we are able to express the overall emission properties of the individual Lhca proteins in terms of emitting dipole moment. Table 4 summarizes all of the observed values and shows the connection between the emission yields calculated from the steady-state emission spectra (Figure 1) and the average fluorescence lifetimes, which were estimated from the globally analyzed time-resolved fluorescence spectra (Table 2) as the value of the emitting dipole moment and normalized to the Chl *a* dipole moment. Table 4 shows that Lhca1 and Lhca2, which do not bind extreme red absorbing pigments,

probably because of the His-ligand they contain instead of the Asn-ligand that Lhca3 and Lhca4 possess in the A5-B5 pigment pair (see more details in refs 11 and 27), have an emitting dipole moment similar to that of LHCII, which also has a His in the A5 binding site, and close to that of a monomeric Chl *a* molecule. In cases where most of the emission originates from the red pigments, that is, in the samples of Lhca3, -4, and the -1/4 dimer, the emitting dipole moments are less than 1, with the lowest value for Lhca4. This suggests that, at room temperature, the red-most state is at least not a super-radiative state. It is also noteworthy that a Gaussian decomposition analysis for the room-temperature absorption spectra of the Lhca samples shows that the red pigments carry the oscillator strength of less than one Chl *a* molecule.¹¹ Even though unequal distribution of the oscillator strength between two (or more) excitonic bands might be expected, the results presented in this study, together with the absorption band-analysis, support the idea that the red (exciton) states are coupled with (dark) charge-transfer state(s), which is a clear outcome of the Stark and pressure-dependent spectroscopic experiments with various PSI particles.^{19,42,44–46} Furthermore, the hypothetical coupling of the red pigments to the carotenoids and their possible influence on the decay lifetimes requires further investigation of samples with various carotenoid compositions.

In our study, all of the samples, which possess red pigments, show an “extra” component with a lifetime of about 50–200 ps in the monomers and about 40 ps in the Lhca1/4 dimer. Global analysis shows that this component is not a typical energy-transfer equilibration component between red and bulk pigments, neither does it display a typical Chl *a* emission spectrum. We assign this compartment to an intermediate state, during which a small structural change of the protein occurs following the excitation, which leads to loss of excitation in the bulk spectrum and which shows a long tail at the red side of the emission spectra (above 800 nm, Figure 5).

Similar components with time-scales of 20–100 ps have been observed in previous studies with Lhca samples, with various (or without any) descriptions.^{20,21,28} Melkozernov et al. found an approximately 20 ps component in reconstituted Lhca1/4 complexes and described it as an intermonomeric energy transfer time.²⁸ Gobets et al. also found a component with about 20 ps and described it as a change in the emitting transition moment.²⁰ Jennings and co-workers found a “slow” 100 ps component in studies with native LHCI and described it as slow energy transfer from the bulk to the red pigments.²¹ In some cases, a similar 100 ps component was also found in time-resolved studies of Lhcb proteins,^{47–50} which lack red pigments. In some studies with LHCII, this component has been described as an artifact that is either due to aggregation of the complexes or due to high excitation powers.⁵⁰ It has also been found in the case of monomeric systems and actually shows up more pronounced in studies with reconstituted systems.^{47,48,51} However, as stated above, in the case of LHCI proteins, a similar component was found in both native and reconstituted systems. It is tempting to consider this loss channel to have the same origin as that found in the native PSI–LHCI particles.^{12,52} The time constant for the loss channel from the Intermediate compartment is about 170 ps for the Lhca1/4 dimer. The Lhca1/4 dimer is considered to be a “natural” dimer in the PSI–LHCI particle. On the basis of the target analysis of time-resolved fluorescence data, the “loss” channel in PSI–LHCI was modeled to be about 150 ps.¹² In principle, the above-mentioned structural rearrangement in the excited state can be very small (on the order of 0.1 Å), and it can be attributed to the formation of an excimer state. Such

an excimer character was proposed previously to explain the emission properties of the red pigments.¹⁹

Except for Lhca1, which does not bind red pigments, monoexponential (average) equilibration times between bulk and red pigments were observed for all samples. The same equilibration time was found, irrespective of the specific energy difference between the bulk and red pigments of each protein (Figure 1). In other studies, multiexponential equilibration times were reported.^{20,31} The time resolution of our experiment was about 5 ps, which (together with the Soret-*Q_y* relaxation times) limits the possibility to observe multiexponential equilibration times. Although fully resolving this issue will require a slightly better time resolution than that achieved in this study, we conclude that the equilibration among the pigments is rather fast and that the spectral overlap is a less important factor for the energy-transfer kinetics in comparison with the distance and orientation of the pigments, which agrees with the fact that the red forms originate from the same binding sites in all Lhca proteins (A5-B5).^{11,27}

Final Remark. Our study shows that Lhca proteins have faster decay lifetimes and lower emission yields compared to their counterparts of PSII antenna proteins, LHCII and CP29. Whether this occurs because of the different pigment composition or the different protein configuration is a topic of future studies. It is notable, however, that the observed “fast” decay lifetimes/low emission yields of Lhca proteins have only a small effect on the overall photochemical yield of PSI because of the much faster trapping times of the PSI reaction center compared to those of PSII.

Acknowledgment. This work was funded by the European Community’s Human Potential Program Grant HPRN-CT-2002-00248 (PSICO) and by Ministero dell’Istruzione Università e Ricerca (MIUR) Progetti Fondo per gli Investimenti della Ricerca di Base (FIRB) Grants RBAU01E3CX and RBNE01LACT by Provincia Autonoma di Trento, progetti liberi. SAMBA per 2. J.A.I is grateful for a grant from the Academy of Finland (Project No. 203824). The authors thank Dr. Miguel Palacios for useful discussions.

References and Notes

- (1) Haworth, P.; Watson, J. L.; Arntzen, C. J. *Biochim. Biophys. Acta* **1983**, *724*, 151–158.
- (2) Jansson, S. *Trends Plant Sci.* **1999**, *4*, 236–240.
- (3) Ganeteg, U.; Klimmek, F.; Jansson, S. *Plant Mol. Biol.* **2004**, *54*, 641–651.
- (4) Boekema, E. J.; Jensen, P. E.; Schlodder, E.; van Breemen, J. F. L.; van Roon, H.; Scheller, H. V.; Dekker, J. P. *Biochemistry* **2001**, *40*, 1029–1036.
- (5) Ben-Shem, A.; Frolow, F.; Nelson, N. *Nature* **2003**, *426*, 630–635.
- (6) Croce, R.; Morosinotto, T.; Castelletti, S.; Breton, J.; Bassi, R. *Biochim. Biophys. Acta* **2002**, *1556*, 29–40.
- (7) Liu, Z.; Hanchi, Y.; Wang, K.; Kuang, T.; Zhang, J.; Gui, L.; An, X.; Chang, W. *Nature* **2004**, *428*, 287–292.
- (8) van Amerongen, H.; van Grondelle, R. *J. Phys. Chem. B* **2001**, *105*, 604–617.
- (9) Novoderezhkin, V. I.; Palacios, M. A.; van Amerongen, H.; van Grondelle, R.; *J. Phys. Chem. B* **2004**, *108*, 10363–10375.
- (10) Novoderezhkin, V.; Palacios, M. A.; van Amerongen, H.; van Grondelle, R. *J. Phys. Chem. B* **2005**, *109*, 10493–10504.
- (11) Morosinotto, T.; Breton, J.; Bassi, R.; Croce, R. *J. Biol. Chem.* **2003**, *278*, 49223–49229.
- (12) Ihalainen, J. A.; van Stokkum, I. H. M.; Gibasiewicz, K.; Germano, M.; van Grondelle, R.; Dekker, J. P. *Biochim. Biophys. Acta* **2005**, *1706*, 267–275.
- (13) Croce, R.; Dorra, D.; Holzwarth, A. R.; Jennings, R. C. *Biochemistry* **2000**, *39*, 6341–6348.
- (14) Gobets, B.; van Stokkum, I. H. M.; Rögner, M.; Kruij, M.; Schlodder, E.; Karapetyan, N. V.; Dekker, J. P.; van Grondelle, R. *Biophys. J.* **2001**, *81*, 407–424.

- (15) Gobets, B.; van Grondelle, R. *Biochim. Biophys. Acta* **2001**, *1507*, 80–99.
- (16) Mukerji, I.; Sauer, K. *Biochim. Biophys. Acta* **1993**, *1142*, 311–320.
- (17) Croce, R.; Zucchelli, G.; Garlaschi, F. M.; Jennings, R. C. *Biochemistry* **1998**, *37*, 17355–17360.
- (18) Ihalainen, J. A.; Gobets, B.; Sznee, K.; Brazzoli, M.; Croce, R.; Bassi, R.; van Grondelle, R.; Korppi-Tommola, J. E. I.; Dekker, J. P. *Biochemistry* **2000**, *39*, 8625–8631.
- (19) Ihalainen, J. A.; Rätsep, M.; Jensen, P. E.; Scheller, H. V.; Croce, R.; Bassi, R.; Korppi-Tommola, J. E. I.; Freiberg, A. *J. Phys. Chem. B* **2003**, *107*, 9086–9093.
- (20) Gobets, B.; Kennis, J. T. M.; Ihalainen, J. A.; Brazzoli, M.; Croce, R.; van Stokkum, I. H. M.; Bassi, R.; Dekker, J. P.; van Amerongen, H.; Fleming, G. R.; van Grondelle, R. *J. Phys. Chem. B* **2001**, *105*, 10132–10139.
- (21) Jennings, R. C.; Zucchelli, G.; Engelmann, E.; Garlaschi, F. M. *Biophys. J.* **2004**, *87*, 488–497.
- (22) Schmid, V. H. R.; Cammarata, K. V.; Bruns, B. U.; Schmidt, G. *W. Proc. Natl. Acad. Sci. U.S.A.* **1997**, *94*, 7667–7672.
- (23) Schmid, V. H. R.; Paulsen, H.; Rupprecht, J. *Biochemistry* **2002**, *41*, 9126–9131.
- (24) Castelletti, S.; Morosinotto, T.; Robert, B.; Caffarri, S.; Bassi, R.; Croce, R. *Biochemistry* **2003**, *42*, 4226–4234.
- (25) Morosinotto, T.; Castelletti, S.; Breton, J.; Bassi, R.; Croce, R. *J. Biol. Chem.* **2002**, *277*, 36253–36261.
- (26) Schmid, V. H. R.; Thome, P.; Ruhle, W.; Paulsen, H.; Kuhlbrandt, W.; Rogl, H. *FEBS Lett.* **2001**, *49*, 27–31.
- (27) Croce, R.; Morosinotto, T.; Ihalainen, J. A.; Chojnicka, A.; Breton, J.; Dekker, J. P.; van Grondelle, R.; Bassi, R. *J. Biol. Chem.* **2004**, *279*, 48543–48549.
- (28) Melkozernov, A. N.; Schmid, V. H. R.; Schmidt, G. W.; Blankenship, R. E. *J. Phys. Chem. B* **1998**, *102*, 8183–8189.
- (29) Melkozernov, A. N.; Schmid, V. H. R.; Lin, S.; Paulsen, H.; Blankenship, R. E. *J. Phys. Chem. B* **2002**, *106*, 4313–4317.
- (30) Melkozernov, A. N.; Lin, S.; Schmid, V. H. R.; Paulsen, H.; Schmidt, G. W.; Blankenship, R. E. *FEBS Lett.* **2002**, *471*, 89–92.
- (31) Gibasiewicz, K.; Croce, R.; Morosinotto, T.; Ihalainen, J. A.; van Stokkum, I. H. M.; Dekker, J. P.; Bassi, R.; van Grondelle, R. *Biophys. J.* **2005**, *88*, 1959–1969.
- (32) Ben-Shem, A.; Frolow, F.; Nelson, N. *Photosynth. Res.* **2004**, *81*, 239–250.
- (33) Weber, G.; Teale, F. W. J. *Trans. Faraday Soc.* **1957**, *53*, 646–655.
- (34) Holzwarth, A. R. In *Biophysical Techniques in Photosynthesis*; Ames, J., Hoff, A. J., Eds.; Kluwer Academic Publishers: Dordrecht, The Netherlands, 1996; pp 75–92.
- (35) van Stokkum, I. H. M.; Larsen, D. S.; van Grondelle, R. *Biochim. Biophys. Acta* **2004**, *1657*, 82–104.
- (36) Palacios, M. A.; de Weerd, F. L.; Ihalainen, J. A.; van Grondelle, R.; van Amerongen, H. *J. Phys. Chem. B* **2002**, *106*, 5782–5787.
- (37) van Amerongen, H.; Valkunas, L.; van Grondelle, R. *Photosynthetic Excitons*; World Scientific: Singapore, 2000; Chapters 2 and 3.
- (38) Berera, R.; Palacios, R.; Vengris, M.; Kódis, G.; van Grondelle, R.; van Amerongen, H.; Gust, D.; Moore, T. A.; Moore, A. L.; Kennis, J. T. M. In *Photosynthesis: Fundamental Aspects to Global Perspectives*; van der Est, A., Bruce, D., Eds.; Alliance Communications Group: Lawrence, KS, 2005; pp 1075–1077.
- (39) Holt, N. E.; Zigmantas, D.; Valkunas, L.; Li, X.-P.; Niyogi, K. K.; Fleming, G. R. *Science* **2005**, *307*, 433–435.
- (40) Peterman, E. J. G.; Wenk, S. O.; Pullertis, T.; Pålsson, L. O.; van Grondelle, R.; Dekker, J. P.; Rögner, M.; van Amerongen, H. *Biophys. J.* **1998**, *75*, 389–398.
- (41) Dashdorj, N.; Zhang, H.; Kim, H.; Yan, J.; Cramer, W. A.; Savikhin, S. *Biophys. J.* **2005**, *88*, 4178–4187.
- (42) Renger, T. *Phys. Rev. Lett.* **2004**, *93*, 188101.
- (43) Carbonera, D.; Agostini, G.; Morosinotto, T.; Bassi, R. *Biochemistry* **2005**, *44*, 8337–8346.
- (44) Rätsep, M.; Johnson, T. W.; Chitnis, P. R.; Small, G. J. *J. Phys. Chem. B* **2000**, *104*, 836–847.
- (45) Zazubovich, V.; Matsuzaki, S.; Johnson, T. W.; Hayes, J. M.; Chitnis, P. R.; Small, G. J. *Chem. Phys.* **2002**, *275*, 47–59.
- (46) Frese, R. N.; Palacios, M. A.; Azzizi, A.; van Stokkum, I. H. M.; Kruij, J.; Rögner, M.; Karapetayan, M. V.; Schlodder, E.; van Grondelle, R.; Dekker, J. P. *Biochim. Biophys. Acta* **2002**, *1554*, 180–191.
- (47) Croce, R.; Müller, M. G.; Bassi, R.; Holzwarth, A. R. *Biophys. J.* **2001**, *80*, 901–915.
- (48) Croce, R.; Müller, M. G.; Caffarri, S.; Bassi, R.; Holzwarth, A. R. *Biophys. J.* **2003**, *84*, 2517–2532.
- (49) Gradinaru, C. C.; Ozdemir, S.; Gulen, D.; van Stokkum, I. H. M.; van Grondelle, R.; van Amerongen, H. *Biophys. J.* **1998**, *75*, 3064–3077.
- (50) Barzda, V.; Gulbinas, V.; Kanavicius, R.; Cervinskis, V.; van Amerongen, H.; van Grondelle, R.; Valkunas, L. *Biophys. J.* **2001**, *80*, 2409–2421.
- (51) Palacios, M. Ph.D. Thesis, Vrije Universiteit Amsterdam, 2005.
- (52) Ihalainen, J. A.; Jensen, P. E.; Haldrup, A.; van Stokkum, I. H. M.; van Grondelle, R.; Scheller, H. V.; Dekker, J. P. *Biophys. J.* **2002**, *83*, 2190–2201.